

Removal of Lead Ions from Aqueous Solution using Zirconium Dioxide Nanoparticles

TAN TAI NGUYEN^{id}

Department of Materials Science, School of Applied Chemistry, Tra Vinh University, Tra Vinh City 87000, Vietnam

Corresponding author: Tel: +84 964896974; E-mail: nttai60@tvu.edu.vn

Received: 17 May 2023;

Accepted: 19 June 2023;

Published online: 6 July 2023;

AJC-21303

This study demonstrated the feasibility of using zirconium dioxide nanoparticles (ZrO₂ NPs) synthesized using a hydrothermal technique for the removal of lead in aqueous solution. The physico-chemical characterization illustrated that the synthesized ZrO₂ NPs have a non-uniform shape with an average size of 15 nm, surface area of 41.56 m² g⁻¹ and adsorption pore width of 3.06 nm. These findings revealed the potential use of ZrO₂ NPs for chelating lead ions. The maximum lead adsorption capacity of ZrO₂ NPs was obtained around 4.12 mg g⁻¹ at adsorption conditions *i.e.*, stirring speed of 200 rpm and contact time of 120 min. Thus, this method provides a number of advantages, including an efficient and cost-effective method for the removal of lead using ZrO₂ NPs.

Keywords: Adsorption, Capacity, Isothermal, Lead ions, Zirconium dioxide nanoparticles.

INTRODUCTION

In order to eliminate the heavy metal ions such Zn²⁺, Cd²⁺, Hg²⁺, Cu²⁺, Pb²⁺ and Fe²⁺, several absorptive materials have been developed extensively over the past few decades [1-5]. Lead(II) ions, more so than any of the other heavy metals described [6-10], are present in both groundwater and surface water and constitute a significant risk to human health. Lead poisoning might create numerous health issues for humans if the water people drink or the crops they eat were tainted with lead [11]. Long-term drinking water containing the high level of Pb²⁺ ions could be caused cancer, Alzheimer's disease, neurodegenerative disease along with metabolism disorders [12-16]. Until now, most of researches has been developed utilizing various techniques for removing of Pb²⁺ ions *i.e.* chemical precipitation coagulation, membrane technology, electrochemical reduction, flocculation and cementation and ion exchange [17-20]. However, it should be noted that those methods have several drawbacks including low capacity for removal, long time for operation, low mechanical and thermal stability [17,19,20].

Among various treatment techniques, the adsorption is a promising technique due to its easy operation and cost-effective process for removal of Pb²⁺ ions from aqueous environment. Therefore, several adsorbents for removal of Pb²⁺ ions has been studied *i.e.*, iron slag, steel slag, fly ash, saw dust activated carbon and agricultural-byproducts [21-28]. Zirconium dioxide

(ZrO₂) exhibits unique features, which make it a suitable adsorbent for Pb²⁺ ion removal, such as being chemically stable during manufacturing, storage and application. This suggests that it could be a desirable adsorbent for use in water purification applications. Few studies have been reported the efficacy of zirconium-based oxides in removing Pb²⁺ ions. Most of the researchers focused on Zr modified polystyrene, Zr combined activated carbon [29,30]. Few reports are reported for the removal of lead from water based on zirconia nanoparticles [31] and the adsorption mechanism of Pb²⁺ by ZrO₂ still remains.

In this study, ZrO₂ nanoparticles (ZrO₂ NPs) was prepared by utilizing a simple hydrothermal process under certain controlled conditions like concentration of NaOH, stirring speed, stirring time and heating time. The physico-chemical properties of ZrO₂ NPs were investigated for applications of removal of Pb²⁺ ions. In addition, the adsorption conditions were optimized based on several factors *i.e.* stirring speed, adsorption time and concentration of adsorbate. The adsorption equilibrium isotherms were fitted using different models (Langmuir and Freundlich) were best described at different concentrations of Pb²⁺ ions.

EXPERIMENTAL

Chemical agents including zirconium oxychloride octahydrate (ZrOCl₂·8H₂O, 99%), sodium hydroxide, nitric acid

(98%), lead (98%) were purchased from Sigma-Aldrich, USA. Diionized water was used throughout the work.

Preparation of ZrO₂ nanoparticles: The ZrO₂ NPs were synthesized using the conventional hydrothermal method. In this work, the synthesized process could be briefly described with four steps. In the first step, ZrOCl₂·8H₂O (4 g) was soaked with 500 mL of NaOH at room temperature and then the mixture was stirred with vigorous stirring in order to initiate the hydrolysis-condensation reaction. The mixture was then filtrated, and the resulting gel was dispersed in ethanol, rinsed three times with diionized water and dried to eliminate any leftover surfactants. The synthesized ZrO₂ NPs was stored in desiccator for future work. In this work, the effect of NaOH concentration, stirring time, stirring speed and heating time were also studied.

Physico-chemical and morphological characterization: Several analytical approaches were used to get the physico-chemical characterization of ZrO₂ NPs and the lead ions adsorption. The transmission electron microscopy (TEM, Keyence VKX-1000) was used for the ultrastructural analysis, while the atomic absorption spectroscopy (AAS, Agilent 240 AAS) was used to estimate the concentration of lead solution. The pore size distribution was obtained by BJH (Micrometrics ASAP 2010), whereas the surface area was measured by the BET method.

Adsorption process: At room temperature, the lead ion adsorption capacity of ZrO₂ NPs was investigated using various parameters. The lead concentration was varied from 2 to 10 mg L⁻¹ and measured using atomic absorption spectroscopy. By regulating an increase of 100 rpm, the effect of stirring speed was explored in the range of 100 to 500 rpm. The contact duration was increased from 60 to 180 min. All the adsorption experiments were carried out at room temperature. The lead adsorption capacity (q_{AC}) was estimated by using eqn. 1 [32,33]:

$$q_{AC} = \frac{C_{in} - C_{fn}}{m_{ZrO_2NPs}} V \quad (1)$$

where C_{in} is the concentration of Pb²⁺ ions at the initial state; C_{fn} is the concentration of Pb²⁺ ions at the equilibrium state. The m_{ZrO₂NPs} is the mass of adsorbent and V is the volume of adsorbate.

RESULTS AND DISCUSSION

In this work, ZrOCl₂·8H₂O (4 g) was used for the conventional hydrothermal synthesis of ZrO₂ nanoparticles. To optimize the conditions for ZrO₂ NPs synthesis, the effect of NaOH concentration, stirring time, stirring speed and heating time were investigated. The heating temperature of 600 °C was maintained during all the process.

Effect of NaOH: The efficiency of ZrO₂ NPs synthesized using different concentrations of NaOH for neutralization is shown in Fig. 1a. The experiments were carried out with different NaOH concentrations of 0.01, 0.05, 0.10, 0.15, 0.20, 0.25 M, and the stirring time, stirring speed, and heating time were set to 240 min, 400 rpm and 300 min, respectively. The results revealed that the concentration of NaOH was proportional to the efficiency. At a NaOH concentration of 0.1 M, the efficiency

of ZrO₂ NPs synthesised was roughly 55%. Thus, it is concluded that by regulating the other parameters, the removal efficiency can be improved.

Effect of stirring time: The stirring time of ZrOCl₂·8H₂O in NaOH solution was set as a series of 120, 180, 240, 300 and 360 min. Fig. 1b showed that the amount of synthesized ZrO₂ NPs was gradually increased, which results an increase in the removal efficiency from 45%, 48% and 52% for 120 min, 180 min and 240 min, respectively. The results showed that amount of ZrO₂ synthesis was saturated at 240 min.

Effect of stirring speed: In order to optimize the condition for the synthesized ZrO₂ NPs, stirring speed was investigated. The experiments were performed with stirring speed series of 200, 300, 400, 500, 600 rpm and the stirring time, concentration of NaOH and heating time were fixed at 240 min, 0.1 M, 300 min, respectively. The results represented that stirring speed was associated to the efficiency. And the efficiency of ZrO₂ NPs synthesised was obtained around 52% at the striring speed of 400 rpm as seen in Fig. 1c.

Effect of heating time: Heating time of synthesized ZrO₂ NPs was set as a series of 180, 240, 300, 360 and 420 min. Fig. 1d showed that the amount of ZrO₂ NPs synthesised was gradually decreased. However, the size of synthesized ZrO₂ NPs was measured by particle size analyer. The results showed that the size of ZrO₂ NPs synthesised was obtained around 90 nm with heating time of 300 min as shown in Table-1. The surface area of synthesized ZrO₂ NPs increases with decreasing size, hence smaller NPs have greater adsorption properties.

TABLE-1
PARTICLE SIZE ANALYZER FOR ZrO₂ NPs
SYNTHESIZED BY CONTROLLING HEATING TIME

Time (min)	180	240	300	360	420
Size (nm)	168.9	134.7	90.6	96.3	109.3

Characterization of ZrO₂ NPs: The EDX spectrum (Fig. 2a) indicates presence of Zr and O elements only which comprised with the weight percent of 50.82% and 28.22%, respectively. A TEM image of synthesized ZrO₂ NPs (Fig. 2b and Fig. 2d) illustrated that the synthesized ZrO₂ NPs were aggregated and the size ranged from few nanometers to around 30 nm with the average size of around 15 nm (Fig. 2c). Moreover, the BET and BJH analysis showed that ZrO₂ NPs proposed a specific surface area of 41.56 m² g⁻¹ with an average pore size of 3.06 nm, leading to provide promising adsorbent for the removal of lead ions.

Effective removal of lead ions

Effect of stirring speed: All the adsorption experiments were conducted using a batchwise approach to examine the impact of stirring speed, contact time and lead ion concentration on lead ion adsorption behaviour. To investigate the impact of stirring rate, 0.025 g of adsorbent was added to 100 mL of aqueous solution containing lead concentraion of 2 mg L⁻¹ and then the mixture solution was stirred at 300 K. The relationship between stirring rate and lead adsorption capacity is depicted in Fig. 3. Upon increasing the stirring speed from 100 to 200

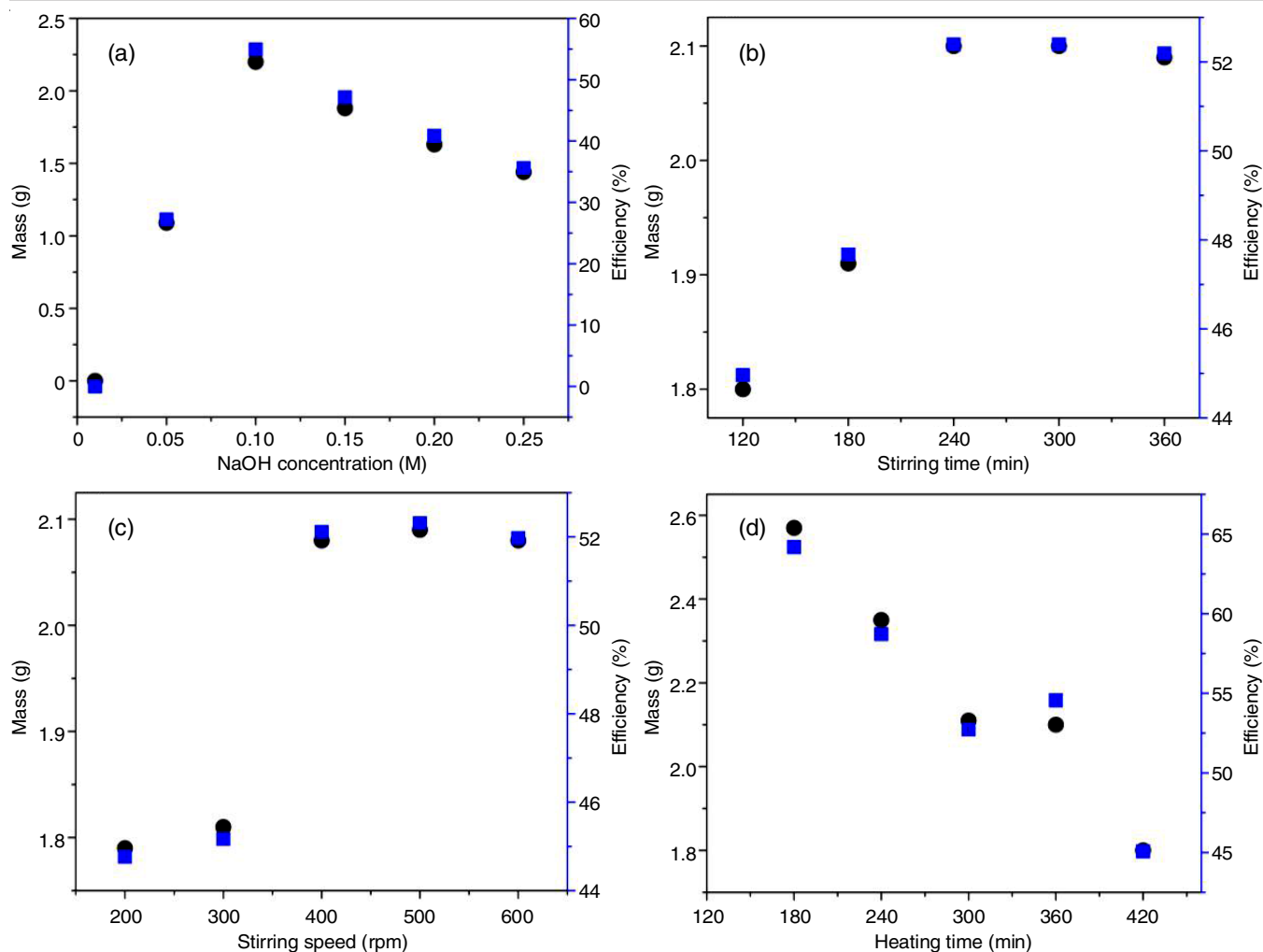


Fig. 1. Experimental results of ZrO₂ NPs synthesized process, (a) effect of sodium hydroxide; (b) effect of stirring time; (c) effect of stirring speed; (d) effect of heating time

rpm enhanced the adsorption capacity. At a stirring speed of 200 rpm, the maximum adsorption value was found to be 8.1 mg g⁻¹. When the stirring speed was increased to over 200 rpm, the lead adsorption capacity decreased. The pores formed during the synthesis of ZrO₂ NPs are a strong contender for understanding the adsorption phenomenon. It should be observed that the smaller the pore size, the more difficult the adsorption. In this case, the pore size of ZrO₂ NPs was achieved around 3.06 nm.

Effect of contact time: A parabolic shape curve with a quadratic second order equation [$q = q_0 + Ax + Bx^2$] was used to fit to the experimental data presented [32]. This is to find an ideal characteristic shape curve for removal of lead ions with various parameters *i.e.* stirring speed and contact time. The estimated results showed that the minimum adsorption capacity of lead (q_0) utilizing ZrO₂ NPs was around 2.38 mg g⁻¹ for stirring speed change (Fig. 3) and 3.06 mg g⁻¹ for contact time change (Fig. 4), respectively. The fitting results also illustrated that the minimum possible adsorption capacity is approximate for both adsorption cases. In addition, all of the correlation coefficients (R^2) for two different cases including effect of contact time and effect of stirring speed were higher than 0.80, as

shown in Table-2. Thus the aforementioned model, a parabolic form curve, adequately described the observed phenomena.

TABLE-2
KINETIC COEFFICIENTS FOR REMOVING LEAD

	Minimum capacity of adsorption q_0 (mg g ⁻¹)	Fitting parameters		
		A (a.u.)	B (a.u.)	R ²
Time	3.06	0.23	-0.01	0.97
Stirring speed	2.38	0.04	-0.0008	0.84

Adsorption isotherms: As can be seen in Fig. 5, the ZrO₂ NPs adsorbed lead ions at a steady rate, reaching a plateau value after 120 min. According to the results of the experiments, an initial adsorption rate of 0.03 mg g⁻¹ min⁻¹ was also attained. It is important to observe that the peak time increases with decreasing adsorption rate. The tiny pore size of 3.06 nm in ZrO₂ NPs is primarily responsible for the weak diffusion of lead ions from the surface adsorption sites to the bulk ZrO₂ NPs pore, which contributes to the relatively low adsorption rate of SiO₂ NPs. The pseudo-first-order kinetic model (eqn. 2) and pseudo-second-order kinetic model (eqn. 3) were also used to investigate the adsorption kinetics [34,35]:

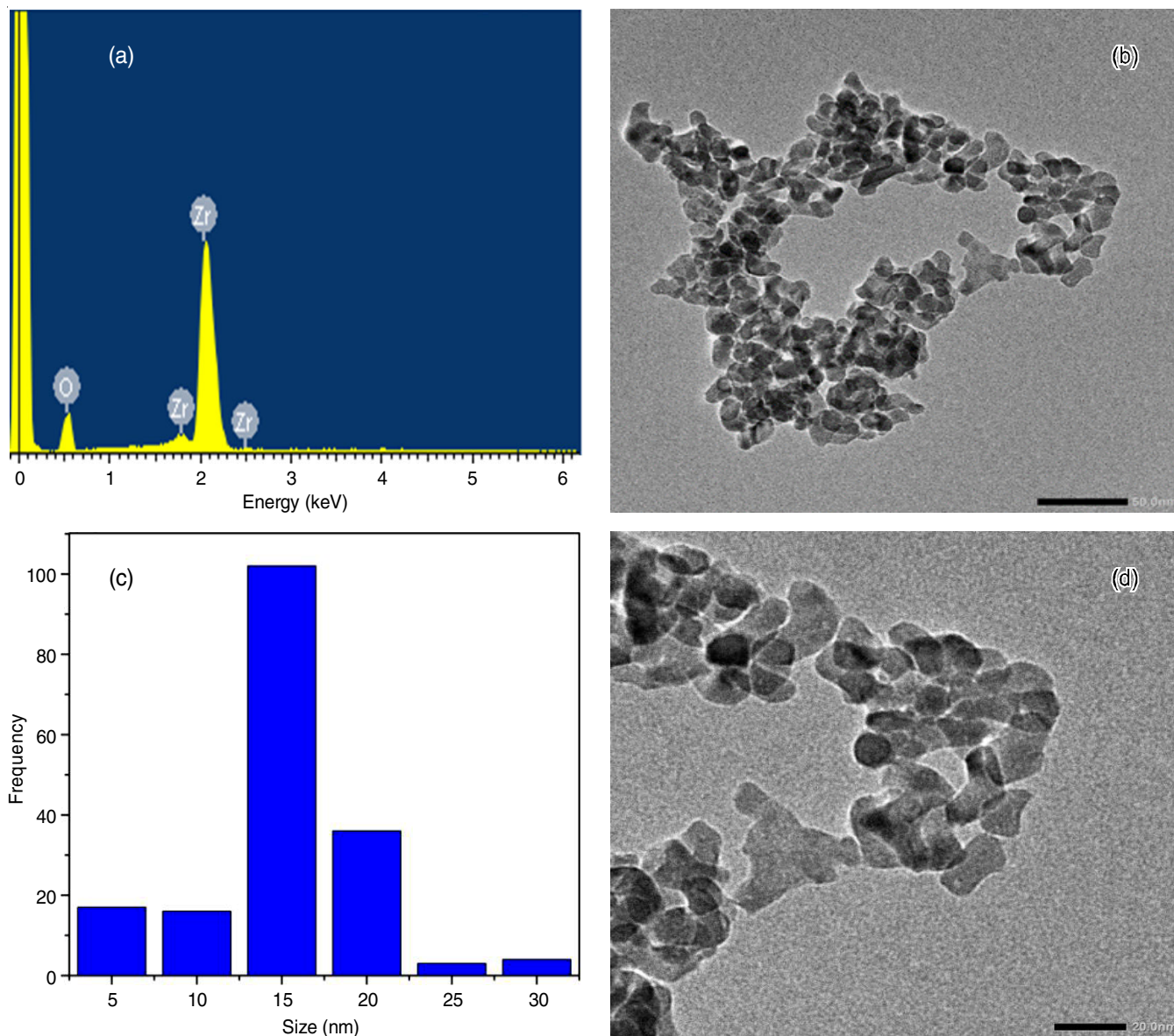


Fig. 2. Characterization of ZrO₂ NPs synthesized, (a) EDS elemental composition analysis of ZrO₂ NPs; (b) TEM image of ZrO₂ NPs; (c) size distribution of ZrO₂ NPs; (d) magnified view of (b)

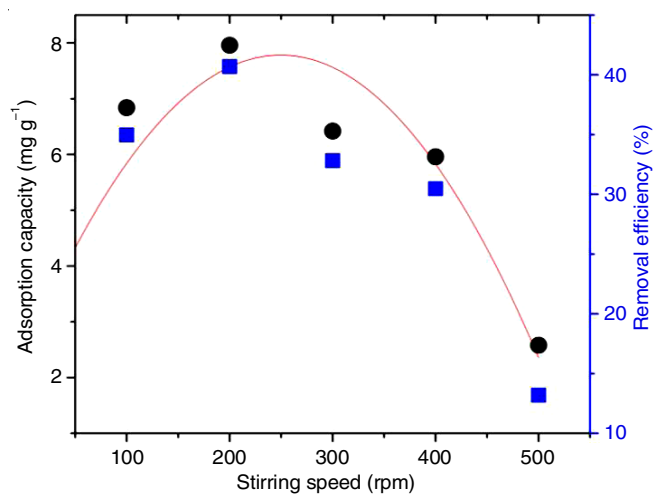


Fig. 3. Influence of stirring speed to the adsorption capacity of lead

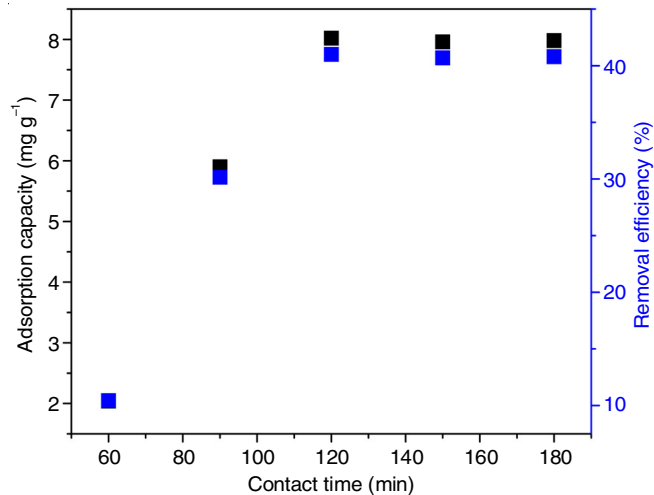
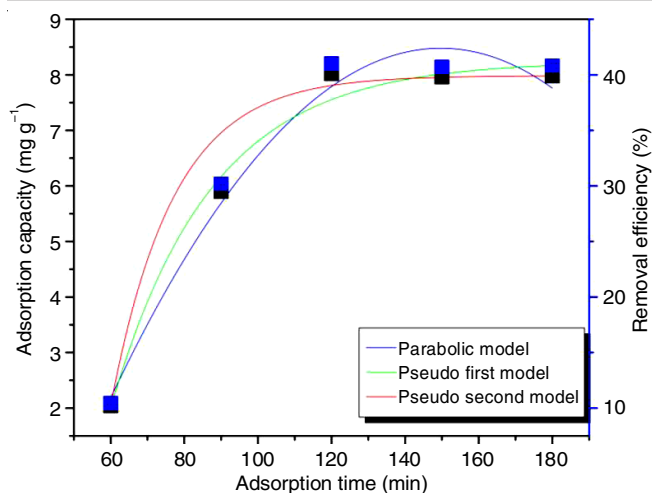


Fig. 4. Effect of contact time to the adsorption capacity of lead

Fig. 5. Adsorption kinetics of lead ions by ZrO₂ NPs

$$q_t = q_{ad} (1 - e^{-T_1 t}) \quad (2)$$

$$q_t = \frac{t}{\frac{1}{T_2 q_{ad}^2} + \frac{t}{q_{ad}}} \quad (3)$$

where q_{ad} and q_t are the adsorption capacity of lead ions at the plateau time and t , respectively, while T_1 and T_2 are the pseudo first and the pseudo second-order rate constants, respectively. Two pseudo-kinetic models, one for mononuclear and one for binuclear adsorption in the solid-liquid system, were presented. The adsorption coefficients that were obtained based on those above equations are shown in Table-3. In addition, Fig. 5 represented a comparison between the parabolic model and both of the pseudo-kinetic models. The adsorption capacity of lead ions was achieved around 8.0 mg g^{-1} , which gives strong agreement with the experimental results. Moreover, the correlation coefficient (R^2) were obtained around 0.97, 0.97 and 0.92 for the case of the parabolic model, the first-pseudo kinetic model and the second-pseudo kinetic model, respectively. These results indicated that both of the adsorption model investigated are suitable to study the kinetic adsorption of lead ions.

The adsorption isotherm models are widely used for the optimization of the adsorption process to design the adsorption model. In this work, the lead ions concentration was set in the range of 2 to 10 mg L^{-1} . Then the experiment was performed

based on the optimizing parameters *i.e.*, stirring speed of 200 rpm and contact time of 120 min at room temperature. The Langmuir (eqn. 4) and Freundlich (eqn. 5) models were used to analyze the experimental data [34,35].

$$C_{eq} = \frac{q_{eq}}{E_L (q_{max} - q_{eq})} \quad (4)$$

$$\log q_{eq} = I \log C_{eq} + \log A_F \quad (5)$$

where C_{eq} , q_{eq} , q_{max} are the concentration of lead ions, the lead ions adsorption capacity at the equilibrium state and the maximum adsorption capacity of lead ions, respectively; E_L is the adsorption energy; I is the adsorption intensity and A_F is the adsorption affinity.

All of the fitting parameters, such as the adsorption factors and correlation coefficients are listed in Table-4. These values were calculated using the Langmuir model (Fig. 6a) and the Freundlich model (Fig. 6b). A low adsorption intensity (I) of 0.31 was found using the Freundlich model, reflecting the slow adsorption rate of the lead ions. This causes an adsorption time that is 120 min longer than it would be without the salt, as seen in Fig. 5. In addition, the affinity between ZrO₂ NPs and lead ions was obtained around 0.95 mg g^{-1} offered low interaction between ZrO₂ NPs surface and lead ions. It is important to take into account that the adsorption of Pb²⁺ ions increased approximately linearly with the increasing E_L values. These calculated values are consistent with the modest initial adsorption rate of $0.03 \text{ mg g}^{-1} \text{ min}^{-1}$. The Langmuir model, in contrast to the theoretically-based Freundlich model, was provided with a maximum lead the adsorption capacity. A probable adsorption capacity of 4.12 mg g^{-1} was predicted using the Langmuir isotherm model (Fig. 6a), which is a better result when compared to the study reported in the literature (Table-5). Furthermore, as compared to the Freundlich isotherm, the model based on the Langmuir isotherm demonstrated a higher correlation coefficient (R^2). This suggests that ZrO₂ NPs may be a useful tool for removing lead ions from the aqueous solution collected from the industrial manufacturing unit.

Comparison of ZrO₂ NPs with other adsorbents: Table-5 represented the lead ions adsorption capacity of ZrO₂ NPs and other adsorbents *i.e.* fly ash, coir and sludge. It can be seen that the possible adsorption capacity of ZrO₂ NPs is better than that of other adsorbents under the similar experimental

TABLE-3
ADSORPTION COEFFICIENTS FOR KINETIC MODELS

	Possible adsorption capacity q_{ad} (mg g^{-1})	Kinetic coefficients		
		T_1 (min^{-1})	T_2 ($\text{g mg}^{-1} \text{ min}^{-1}$)	R^2
Pseudo-first-order model	8.25	0.04	–	0.97
Pseudo-second-order model	7.46	–	0.01	0.92

TABLE-4
PARAMETERS OF ADSORPTION ISOTHERM FOR REMOVAL OF LEAD

	Maximum adsorption capacity q_{max} (mg g^{-1})	Isotherm coefficients			
		A_F (mg g^{-1})	I	E_L (L mg^{-1})	R^2
Freundlich isotherm	–	0.95	0.31	–	0.76
Langmuir isotherm	4.12	–	–	0.04	0.84

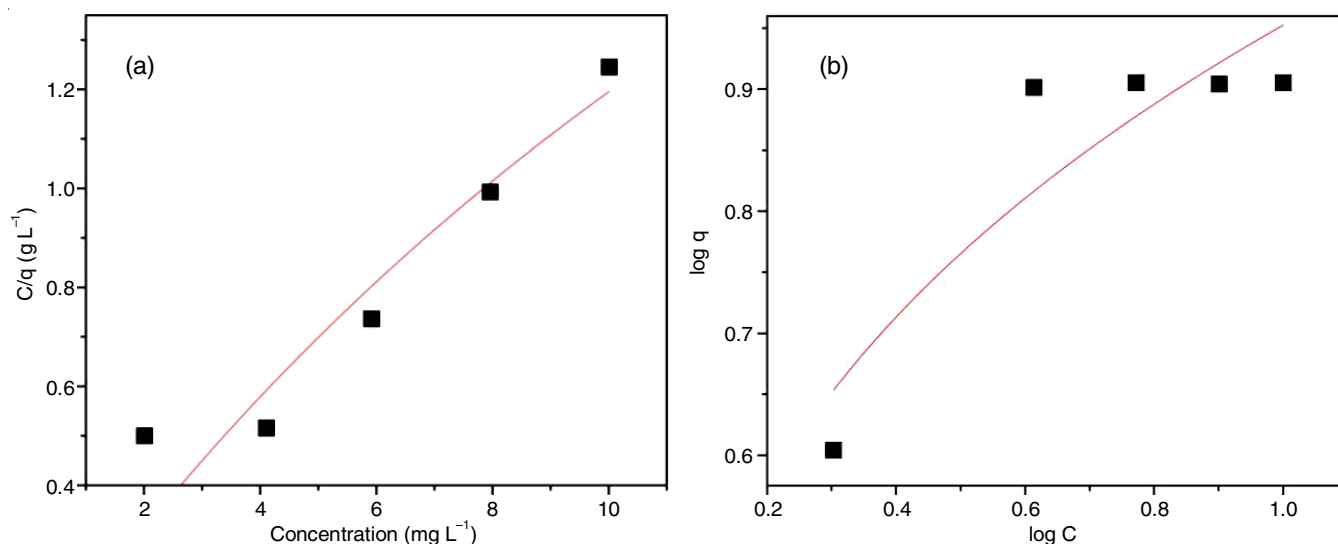


Fig. 6. Langmuir isotherm model (a) and Freundlich isotherm model (b) for removal of lead utilizing ZrO₂ NPs

TABLE-5
COMPARISON OF LEAD ION ADSORPTION
BETWEEN ZrO₂ NPs AND ANOTHER ADSORBENTS

Adsorbents	Concentration range (mg L ⁻¹)	Adsorption capacity (mg g ⁻¹)	Ref.
ZrO ₂	2-10	4.12	This study
Fly ash	5-7	2.50	[22]
Coir	116	0.127	[36]

conditions. In addition, the adsorption capacity of ZrO₂ NPs may enhance based on conjugation with various functional groups for specific detection of heavy metal ions (Cr⁶⁺, Cu²⁺, Pb²⁺) for the environmental applications.

Conclusion

In conclusion, this work represented the synthesis process of zirconium dioxide nanoparticles (ZrO₂ NPs) under different conditions including NaOH concentration, stirring time, stirring speed and heating time. The physico-chemical characterization showed that ZrO₂ NPs were successfully synthesized with an average size of 15 nm; efficiency of around 50%; purity of 100% and surface area of 41.56 m² g⁻¹, leading to efficient removal of lead ions. Consequently, lead ions adsorption capacity of ZrO₂ NPs was investigated under different conditions *i.e.*, stirring speed, contact time and adsorbate concentration. The experimental results illustrated that the maximum adsorption capacity of 4.12 mg g⁻¹ was obtained at stirring speed of 200 rpm, contact time of 120 min for Pb²⁺ ions. In addition, the adsorption capacity could be enhanced by utilizing surface functionalization of ZrO₂ NPs with the functional groups.

ACKNOWLEDGEMENTS

The research was made possible through the Basic Science Research programme at Tra Vinh University, Vietnam.

CONFLICT OF INTEREST

The authors declare that there is no conflict of interests regarding the publication of this article.

REFERENCES

- D.L. Gutnick and H. Bach, *Appl. Microbiol. Biotechnol.*, **54**, 451 (2000); <https://doi.org/10.1007/s002530000438>
- G. Renard, M. Muresanu On leave from the Faculty, A. Galarneau, D.A. Lerner and D. Brunel, *New J. Chem.*, **29**, 912 (2005); <https://doi.org/10.1039/b500302b>
- M. Muresanu, N. Cioatera, I. Trandafir, I. Georgescu, F. Fajula and A. Galarneau, *Micropor. Mesopor. Mater.*, **146**, 141 (2011); <https://doi.org/10.1016/j.micromeso.2011.04.026>
- F. Ge, M.-M. Li, H. Ye and B.-X. Zhao, *J. Hazard. Mater.*, **211-212**, 366 (2012); <https://doi.org/10.1016/j.jhazmat.2011.12.013>
- F. Ke, L.G. Qiu, Y.P. Yuan, F.M. Peng, X. Jiang, A.J. Xie, Y.H. Shen and J.F. Zhu, *J. Hazard. Mater.*, **196**, 36 (2011); <https://doi.org/10.1016/j.jhazmat.2011.08.069>
- B. Volesky and Z.R. Holan, *Biotechnol. Prog.*, **11**, 235 (1995); <https://doi.org/10.1021/bp00033a001>
- K.K. Wong, C.K. Lee, K.S. Low and M.J. Haron, *Chemosphere*, **50**, 23 (2003); [https://doi.org/10.1016/S0045-6535\(02\)00598-2](https://doi.org/10.1016/S0045-6535(02)00598-2)
- A. Kapoor, T. Viraraghavan and D.R. Cullimore, *Bioresour. Technol.*, **70**, 95 (1999); [https://doi.org/10.1016/S0960-8524\(98\)00192-8](https://doi.org/10.1016/S0960-8524(98)00192-8)
- W. Lo, H. Chua, K.H. Lam and S.P. Bi, *Chemosphere*, **39**, 2723 (1999); [https://doi.org/10.1016/S0045-6535\(99\)00206-4](https://doi.org/10.1016/S0045-6535(99)00206-4)
- C.L. Ake, K. Mayura, H. Huebner, G.R. Bratton and T.D. Phillips, *J. Toxicol. Environ. Health A*, **63**, 459 (2001); <https://doi.org/10.1080/152873901300343489>
- A.L. Wani, A. Ara and J.A. Usmani, *Interdiscip. Toxicol.*, **8**, 55 (2015); <https://doi.org/10.1515/intox-2015-0009>
- K. Steenland and P. Boffetta, *Am. J. Ind. Med.*, **38**, 295 (2000); [https://doi.org/10.1002/1097-0274\(200009\)38:3<295::AID-AJIM8>3.0.CO;2-L](https://doi.org/10.1002/1097-0274(200009)38:3<295::AID-AJIM8>3.0.CO;2-L)
- C. Wallin, S.B. Sholts, N. Österlund, J. Luo, J. Jarvet, P.M. Roos, L. Ilag, A. Gräslund and S.K.T.S. Wärmländer, *Sci. Rep.*, **7**, 14423 (2017); <https://doi.org/10.1038/s41598-017-13759-5>
- L. Charlet, Y. Chapron, P. Faller, R. Kirsch, A.T. Stone and P.C. Baveye, *Coord. Chem. Rev.*, **256**, 2147 (2012); <https://doi.org/10.1016/j.ccr.2012.05.012>
- P. Zatta, D. Drago, S. Bolognin and S.L. Sensi, *Trends Pharmacol. Sci.*, **30**, 346 (2009); <https://doi.org/10.1016/j.tips.2009.05.002>
- S. Coon, A. Stark, E. Peterson, A. Gloi, G. Kortsha, J. Pounds, D. Chettle and J. Gorell, *J. Environ. Health Perspect.*, **114**, 1872 (2006); <https://doi.org/10.1289/ehp.9102>

17. Y. Liu, H. Wang, Y. Cui and N. Chen, *Int. J. Environ. Res. Public Health*, **20**, 3885 (2023); <https://doi.org/10.3390/ijerph20053885>
18. S.W. Lin and R.M.F. Navarro, *Chemosphere*, **39**, 1809 (1999); [https://doi.org/10.1016/S0045-6535\(99\)00074-0](https://doi.org/10.1016/S0045-6535(99)00074-0)
19. A. Saeed, M. Iqbal and M.W. Akhtar, *J. Hazard. Mater.*, **117**, 65 (2005); <https://doi.org/10.1016/j.jhazmat.2004.09.008>
20. S. Doyurum and A. Celik, *J. Hazard. Mater.*, **138**, 22 (2006); <https://doi.org/10.1016/j.jhazmat.2006.03.071>
21. Q. Feng, Q. Lin, F. Gong, S. Sugita and M. Shoya, *J. Colloid Interface Sci.*, **278**, 1 (2004); <https://doi.org/10.1016/j.jcis.2004.05.030>
22. V.K. Gupta and I. Ali, *J. Colloid Interface Sci.*, **271**, 321 (2004); <https://doi.org/10.1016/j.jcis.2003.11.007>
23. P. Chen, J. Wu, L. Li, Y. Yang and J. Cao, *Appl. Surf. Sci.*, **624**, 157165 (2023); <https://doi.org/10.1016/j.apsusc.2023.157165>
24. A.A. Alghamdi, A.B. Al-Odayni, W.S. Saeed, A. Al-Kahtani, F.A. Alharthi and T. Ouak, *Materials*, **12**, 2020 (2019); <https://doi.org/10.3390/ma12122020>
25. K.A. Krishnan, A. Sheela and T.S. Anirudhan, *J. Chem. Technol. Biotechnol.*, **78**, 642 (2003); <https://doi.org/10.1002/jctb.832>
26. K.G. Sreejalekshmi, K.A. Krishnan and T.S. Anirudhan, *J. Hazard. Mater.*, **161**, 1506 (2009); <https://doi.org/10.1016/j.jhazmat.2008.05.002>
27. E. Pehlivan, T. Altun, S. Cetin and M. Iqbal Bhanger, *J. Hazard. Mater.*, **167**, 1203 (2009); <https://doi.org/10.1016/j.jhazmat.2009.01.126>
28. N. Kannan and T.E. Veemaraj, *E-J. Chem.*, **6**, 247 (2009); <https://doi.org/10.1155/2009/515178>
29. G. Sharma and M. Naushad, *J. Mol. Liq.*, **310**, 113025 (2020); <https://doi.org/10.1016/j.molliq.2020.113025>
30. Q. Zhang, Q. Du, M. Hua, T. Jiao, F. Gao and B. Pan, *Environ. Sci. Technol.*, **47**, 6536 (2013); <https://doi.org/10.1021/es400919t>
31. A.F.V. da Silva, A.P. Fagundes, D.L.P. Macuvele, E.F.U. de Carvalho, M. Durazzo, N. Padoin, C. Soares and H.G. Riella, *Colloids Surf. A Physicochem. Eng. Asp.*, **583**, 123915 (2019); <https://doi.org/10.1016/j.colsurfa.2019.123915>
32. N. Hoang Lam, H.T. Ma, M.J. Bashir, G. Eppe, P. Avti and T.T. Nguyen, *Int. J. Environ. Anal. Chem.*, **101**, 2668 (2021); <https://doi.org/10.1080/03067319.2019.1708907>
33. T.T. Nguyen, H.T. Ma, P. Avti, M.J.K. Bashir, C.A. Ng, L.Y. Wong, H.K. Jun, Q.M. Ngo and N.Q. Tran, *J. Anal. Methods Chem.*, **2019**, 6210240 (2019); <https://doi.org/10.1155/2019/6210240>
34. P.K. To, H.T. Ma, L. Nguyen Hoang and T.T. Nguyen, *J. Chem.*, **2020**, 8861423 (2020); <https://doi.org/10.1155/2020/8861423>
35. T.T. Nguyen, *J. Chem.*, **2022**, 9944126 (2022); <https://doi.org/10.1155/2022/9944126>
36. S.R. Shukla and R.S. Pai, *J. Chem. Technol. Biotechnol.*, **80**, 176 (2005); <https://doi.org/10.1002/jctb.1176>